# Can the agricultural AquaCrop model simulate water use and yield of a poplar short-rotation coppice?

JOANNA A. HOREMANS[1] (iD), HANNE VAN GAELEN[2], DIRK RAES[2], TERENZIO ZENONE[1] and REINHART CEULEMANS[1]

[1]Department of Biology, Centre of Excellence PLECO, University of Antwerp, Universiteitsplein 1, B-2610 Wilrijk, Belgium, [2]Department of Earth and Environmental Science, K.U.Leuven University, Celestijnenlaan 200E, B-3001 Leuven, Belgium

## Abstract

We calibrated and evaluated the agricultural model AquaCrop for the simulation of water use and yield of a short-rotation coppice (SRC) plantation with poplar (*Populus*) in East Flanders (Belgium) during the second and the third rotation (first 2 years only). Differences in crop development and growth during the course of the rotations were taken into account during the model calibration. Overall, the AquaCrop model showed good performance for the daily simulation of soil water content ($R^2$ of 0.57–0.85), of green canopy cover ($R^2 > 0.87$), of evapotranspiration (ET; $R^2 > 0.76$), and of potential yield. The simulated, total yearly water use of the SRC ranged between 55% and 85% of the water use of a reference grass ecosystem calculated under the same environmental conditions. Crop transpiration was between 67% and 93% of total ET, with lower percentages in the first than in the second year of each rotation. The observed (dry mass) yield ranged from 6.61 to 14.76 Mg ha$^{-1}$ yr$^{-1}$. A yield gap of around 30% was observed between the second and the third rotation, as well as between simulated and observed yield during the third rotation. This could possibly be explained by the expansion of the understory (weed) layer; the relative cover of understory weeds was 22% in the third year of the third rotation. The agricultural AquaCrop model simulated total water use and potential yield of the operational SRC in a reliable way. As the plantation was extensively managed, potential effects of irrigation and/or fertilization on ET and on yield were not considered in this study.

*Keywords:* bioenergy, harvestable biomass prediction, POPFULL, *Populus*, soil water content, yield gap

## Introduction

Short-rotation woody crops (SRCs, cfr. abbreviations in Table 1) with fast-growing trees are a very promising option for the generation of renewable bioenergy (AEBIOM, 2012). They have high energy-use efficiency (Boehmel *et al.*, 2008) and can mitigate greenhouse gas emissions (Adler *et al.*, 2007; Don *et al.*, 2011; Njakou Djomo *et al.*, 2011; Njakou Domo *et al.*, 2013). In comparison with other candidate energy crops, perennial lignocellulosic crops promote biodiversity in an agricultural landscape (Verheyen *et al.*, 2014), enhance soil organic carbon storage (Baum *et al.*, 2009; Don *et al.*, 2011; Berhongaray *et al.*, 2016), and improve groundwater quality (Dimitriou *et al.*, 2009). In the temperate zones of Europe, poplar (*Populus*) is the most suitable genus for SRC plantations (Dillen *et al.*, 2010), but several studies attributed high water consumption to poplar (Zsuffa *et al.*, 1996; Meiresonne *et al.*, 1999). Some of these studies suggested potential reductions of water

table levels and aquifer recharge when extensive SRCs with poplar are established in agricultural areas (Allen *et al.*, 1999; Perry *et al.*, 2001; Hall, 2003; Petzold *et al.*, 2010). These observations have been contradicted by a number of more recent studies (Fischer *et al.*, 2013, 2015; Schmidt-Walter *et al.*, 2014; Zenone *et al.*, 2015), which reported that evapotranspiration (ET) of poplar SRCs did not exceed the reference ET of a well-watered grassland (ET$_0$) under identical climatological conditions. Obviously, the accurate quantification of the water consumption remains a crucial aspect for the development of poplar SRC and for the conversion of agricultural land into these plantations.

There is a similar need to accurately simulate biomass production and the corresponding energy which can be generated under different climate conditions, site characteristics and/or management options (Headlee *et al.*, 2013). For an efficient assessment of the growth, productivity, and water consumption of SRCs, one can rely on various models, ranging from purely empirical models (Ayllot *et al.*, 2008) to process-based forest models (Ceulemans, 1996; Deckmyn *et al.*, 2004; Kollas *et al.*, 2009; Hart *et al.*, 2015). The latter allow to make

Correspondence: Joanna A. Horemans, tel. + 32 3265 1724, fax + 32 3265 2271, e-mail: Joanna.Horemans@uantwerpen.be

**Table 1** Description of abbreviations, symbols, and variables used in this contribution

| Variable | Description | Units |
|---|---|---|
| AGB | Aboveground biomass production | Mg ha$^{-1}$ yr$^{-1}$ |
| $B$ | Total (above- and belowground) biomass production | Mg ha$^{-1}$ yr$^{-1}$ |
| BGB | Belowground biomass production | Mg ha$^{-1}$ yr$^{-1}$ |
| CC | Green canopy cover | % |
| CDs | Calender days | |
| EC | Eddy covariance | |
| $E_{soil}$ | Soil evaporation | mm |
| $E_{soil,tot}$ | Total annual soil evaporation | mm |
| $ET_0$ | Reference crop evapotranspiration | mm |
| $ET_{0,tot}$ | Total annual reference crop evapotranspiration | mm |
| ET | Evapotranspiration | mm |
| $ET_{diff}$ | Difference of ET between two successive days | mm |
| $ET_{tot}$ | Total annual evapotranspiration | mm |
| $G$ | Soil heat flux | W m$^{-2}$ |
| GDDs | Growing degree days | |
| $H$ | Sensible heat flux | W m$^{-2}$ |
| LAI | Leaf area index | dimensionless |
| LE | Latent heat flux | W m$^{-2}$ |
| MAD | Mean absolute deviation | |
| NRMSE | Normalized root-mean-square error | % |
| $PAR_i$ | Incoming photosynthetically active radiation | W m$^{-2}$ |
| $PAR_t$ | Transmitted photosynthetically active radiation | W m$^{-2}$ |
| Pr | Precipitation | mm |
| $Pr_{tot}$ | Total annual precipitation | mm |
| $R^2$ | Coefficient of determination | |
| RC | Relative leaf cover of weeds | % |
| RH | Relative humidity | % |
| RME | Random measurement error | |
| $R_n$ | Net radiation | W m$^{-2}$ |
| $R_s$ | Short-wave radiation | W m$^{-2}$ |
| SRC | Short-rotation woody crop | |
| SWC | Soil water content | mm |
| SWT | Soil water table depth | m |
| $T_{air}$ | Average air temperature | °C |
| $T_{max}$ | Maximum air temperature | °C |
| $T_{min}$ | Minimum air temperature | °C |
| Tr | Transpiration (component of evapotranspiration) | mm |
| $Tr_{tot}$ | Total annual transpiration | mm |
| $u$ | Wind speed | m s$^{-1}$ |
| $Y$ | Yield production = harvestable part of $B$ | Mg ha$^{-1}$ yr$^{-1}$ |

predictions under the future climate conditions and for different sites (Matala *et al.*, 2003) as well as under different management regimes (Korzukhin *et al.*, 1996). These models are, however, often complex and parameter rich. Consequently, they require a vast amount of data for input and parameterization that are not always available (Sands *et al.*, 2000; Larocque *et al.*, 2014). Therefore, the direct use of these models by the end-users – including land use managers, stakeholders of the bioenergy industry, and policy makers – is often restricted (Mohren & Burkhart, 1994; Matala *et al.*, 2003). As SRCs are intensively managed, crop models could be a valuable alternative for forest models to simulate growth, water use, and productivity of SRC. However, in contrast to annual (agricultural) crops, the effect of coppice must be taken into consideration, as well as the recurrent changes in the crop development and in the structure of the SRC within each rotation (Deckmyn *et al.*, 2004; Broeckx *et al.*, 2015; Zenone *et al.*, 2015) and the diversity of poplar species and genotypes (Ceulemans & Deraedt, 1999; Tallis *et al.*, 2013).

The AquaCrop model is a simplified process-based model that simulates soil water content (SWC), crop water use, crop growth, total biomass production (*B*), and yield (*Y*) under different climatological and environmental conditions as well as under different management practices (Raes *et al.*, 2009; Steduto *et al.*, 2009). In AquaCrop, the biophysical processes are simplified so that the amount of data needed for input and for calibration remains limited, while robustness and accuracy are safeguarded (Vanuytrecht *et al.*, 2014b). AquaCrop was initially developed for herbaceous food crops, although forage/feed crops are currently being considered (Kim & Kaluarachchi, 2015). Attempts to use AquaCrop for woody crops are limited to a simulation study of crop transpiration (Tr) of jatropha (Segerstedt & Bobert, 2013) and a study using the water stress function for olive trees (Rallo *et al.*, 2012). Furthermore, good results were obtained for the estimation of leaf biomass in tea plantations (Elbehri *et al.*, 2015). Our first modelling attempts with AquaCrop for a single-stem poplar SRC were previously published (Bloemen *et al.*, 2016).

In view of the need of user-friendly tools for water use and yield prediction of SRCs, this study aimed (i) to evaluate the potential of the agricultural model AquaCrop to simulate both water use and harvestable biomass production of SRCs and (ii) to explore the need for further development of the AquaCrop model for the modelling of perennial woody crops. The stand-level ET, the crop development, and the yield, measured on an operational poplar SRC plantation in East Flanders, Belgium, were used for model evaluation.

## Materials and methods

### Layout and management of experimental plantation

The operational poplar SRC plantation, covering an area of 14.5 ha, was located in Lochristi, East Flanders, Belgium

(51°06′44″N, 3°51′02″E, 6.25 m a.s.l.). The area is characterized by a temperate climate with mild winters and cool summers, with rainfall uniformly spread throughout the year. Before the establishment of the SRC plantation, the site was partly cultivated with agricultural crops (sugar beet, corn) and partly used as pasture land. Hardwood cuttings from 12 different *Populus* genotypes representing four parentages and interspecific hybrids were planted in April 2010. Cuttings were planted in a double-row design with a density of 8000 plants ha$^{-1}$, i.e. 1.1 m within the rows and alternating distances of 0.75 and 1.5 m between the rows (Broeckx *et al.*, 2012). For the first two rotations, the plantation was coppiced after 2 years each. The third rotation was prolonged to 3 years. The first 2 years after plantation establishment (2010–2011; R1.1–R1.2) were not considered in this study. The study period consisted of the entire second rotation (2012–2013; R2.1–R2.2) and the first 2 years of the third rotation (2014–2015; R3.1–R3.2). Both rotations were characterized by multistem stumps (with an average of 10 stems per stump; Verlinden *et al.*, 2015). The crop structure, as well as the observed yield, and some basic properties are presented in Fig. 1.

Neither fertilization nor irrigation was applied during the entire study period. During the first month after planting and after each coppice, conventional manual and chemical SRC weed control (Ledin & Willebrand, 1996) was applied. More information about the design and the management of the plantation has been previously published (Broeckx *et al.*, 2012; Verlinden *et al.*, 2013).

## Meteorological and evapotranspiration measurements

Meteorological data were recorded at half-hourly time steps at the plantation. Air temperature ($T_{air}$) and relative humidity (RH) were measured by Vaisala probes (model HMP45C; Vaisala, Helsinki, Finland) and wind speed ($u$) with a sonic anemometer (model CSAT3; Campbell Scientific, Logan, UT, USA). Incoming short-wave radiation ($R_s$) was monitored with a pyranometer (model CNR1; Kipp & Zonen, Delft, the Netherlands). Daily precipitation (Pr) records were acquired from a nearby meteorological station of the Royal

Meteorological Institute in Zelzate (51°10′53″N, 3°48′33″E, 87.19 m a.s.l.).

Ecosystem-level fluxes of carbon, water, and energy were continuously monitored from an eddy covariance (EC) mast at the plantation. In this study, only water and energy fluxes were considered. High-frequency (10 Hz) measurements of the three-dimensional wind speed components were made using a sonic anemometer. Vertical wind velocity was combined with measurements from a closed-path, fast-response gas analyser (model LI-7000; Li-Cor, Lincoln, NE, USA) to measure the latent heat flux (LE; Bloemen *et al.*, 2016). The LE measurements were aggregated to daily LE values and converted to ET. Additionally, sensible heat ($H$) fluxes were derived from vertical wind speed and sonic temperature measurements. The LE and $H$ fluxes and momentum were calculated from half-hourly aggregates of the high-frequency measurements using the EDIRE software (R. Clement, University of Edinburgh, UK; http://www.geos.ed.ac.uk/abs/research/micromet/Ed iRe/). Gap filling of the original EC data was carried out by the Marginal Distribution Sampling method (Reichstein *et al.*, 2005; Lasslop *et al.*, 2010) using the standard online tool of Fluxnet (http://www.bgc-jena.mpg.de~MDIwork/eddyproc/). More detailed information about the EC measurements at the site has been previously provided (Zona *et al.*, 2013; Zenone *et al.*, 2015).

## Soil measurements

In March 2010, just before planting, a detailed soil analysis was performed. The particle size distribution indicated a loamy sand soil with on average 85.7% sand and 11.3% clay (Verlinden *et al.*, 2013). The volumetric SWC was continuously monitored at 0.2, 0.3, 0.4, 0.6, and 1 m below the soil surface from the start of the plantation (R1.1) until R3.1 and at 0.05, 0.1, 0.2, 0.5, and 1 m below the soil surface for R3.2, using soil moisture probes (TDR model CS616; Campbell Scientific). Soil water table depth (SWT) was monitored using a pressure transducer (model PDCR 1830; Campbell Scientific). The SWC and SWT were measured at five randomly chosen locations in the vicinity of the technical cabin on the plantation. These locations
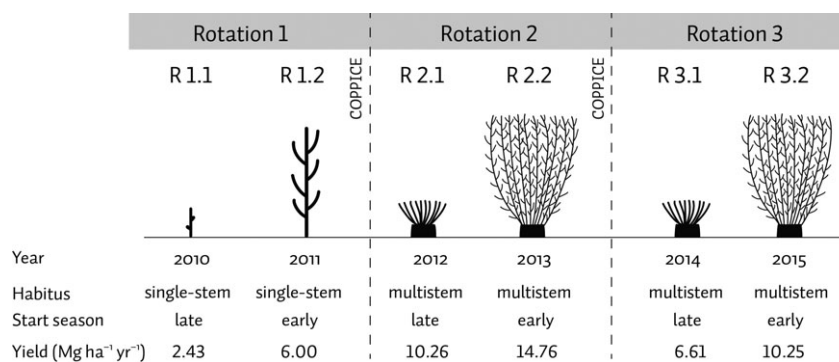


**Fig. 1** Schematic representation of the crop structure during the three rotations of the short-rotation poplar plantation in East Flanders (Belgium). A short description of each year of the first rotation (2010–2011; R1.1–R1.2) and of the second rotation (2012–2013; R2.1–R2.2) and the first 2 years of the third rotation (2014–2015; R3.1–R3.2), in terms of habitus, start of the growing season and observed yield, is also presented.

remained the same over the whole study period. The soil water sensors were changed in R3.2 as the site, a former Fluxnet site (https://fluxnet.ornl.gov) used in the POPFULL project (http://uahost.uantwerpen.be/popfull), became an ICOS site and started following the protocols as described by ICOS (https://www.icos-ri.eu). Analysis of soil samples collected in 2010 and 2014 showed that after 4 years the P, K, Ca, and Mg concentrations in the soil had not significantly changed as compared to the plantation year, and the N concentration in the top soil (0.3–0.6 m) had increased (Vanbeveren *et al.*, 2016b). Soil heat flux ($G$) was continuously measured by eight heat flux plates in the soil (HFT3; REBS Inc., Seattle, WA, USA) at 6–8 cm depth (Zona *et al.*, 2013).

## Assessment of uncertainty on evapotranspiration

The random measurement error (RME) on the aggregated daily ET data was estimated using a method inspired by the 24-h approach described by Hollinger & Richardson (2005). Consecutive measurement pairs with a difference in $ET_0$ larger than 0.6 mm where excluded from the data set, leaving 72.6% of the data, being 1060 data pairs over the 4 years (2012–2015) of the study. For 10 equally sized groups, grouped according to the size of the ET values, the corresponding RME was calculated as the mean absolute deviation (MAD) of the differences in ET ($ET_{diff}$) between successive days. The MAD was used because the distribution of $ET_{diff}$ was not Gaussian (Shapiro–Wilk: 0.87, $P > 0.0001$, Kolmogorov–Smirnov: 0.14, $P < 0.01$, kurtosis: 9.16, and skewness: 0.036), but double exponential (Laplace). Afterwards, a logarithmic function was fitted through the MAD values as a function of the ET ($0.0609 \times (\ln (ET) + 0.209)$). This function was used to calculate the RME on all daily ET values. RME was calculated with SAS statistical software (version 9.1; SAS Institute Inc., Cary, NC, USA). Another source of uncertainty, the energy balance closure of the EC data, was assessed by the calculation of the regression line between the sum of the measured turbulent fluxes $H + LE$ and the available energy $Rn - G$ ($Rn$: net radiation; Foken, 2008; Wohlfahrt *et al.*, 2010).

## Plant and crop measurements

Crop development was monitored by leaf area index (LAI) measurements using a LAI-2200 device (LI-2200; Li-Cor). Four replicate LAI measurements were taken per genotype and per former land use type, and measurements were repeated 11–15 times over the growing season (Broeckx *et al.*, 2015). The LAI measuring device also gave the amount of transmitted ($PAR_t$) and incoming photosynthetically active radiation ($PAR_i$) below the canopy. No LAI measurements were available for R3.1.

The aboveground biomass (AGB) was determined from destructive sampling of stems after the coppice of R1 (10 stems per genotype) and R2 (eight stems per genotype). The stems were oven-dried in the laboratory for 10 days at 70 °C. Afterwards, genotype-specific allometric (quadratic) relations were obtained between the stem biomass and the stem diameter (Verlinden *et al.*, 2013, 2015). Subsequently, the allometric relations were used to calculate the AGB of the poplars for the years without coppice (Broeckx *et al.*, 2012; Verlinden *et al.*, 2015).

Oven-dried belowground woody biomass (BGB) was determined by the excavation of the root system (up to 0.6 m depth) and the stump for two genotypes (Koster and Skado) after the coppice of R1 (20 trees) and R2 (6 trees). The values were scaled up to the plantation level taking into account the planting density and the mortality. For fine root sampling, sequential soil cores (between 10 and 20 samples depending on the expected intrinsic variability of the fine root biomass) were taken during rotation years R1.2 and R2.1 and their dry biomass was quantified (Berhongaray *et al.*, 2013, 2015).

## The AquaCrop model

AquaCrop simulates crop's $B$ and $Y$ using a four-step process. In the first step, the green canopy cover (CC), giving the fraction of the soil covered by green canopy, is simulated. The expansion of CC, from the initial CC ($CC_0$) to the maximum CC ($CC_x$), is described by a type of logistic function determined by the canopy growth coefficient (CGC). AquaCrop parameters and symbols are summarized in Table 2. Canopy senescence at the end of the growing season is described by means of the canopy decline coefficient (CDC). In the second step, Tr is simulated considering $ET_0$, a soil water stress coefficient ($K_s$) and the crop transpiration coefficient ($K_{cTr}$) (Eqn 1). This $K_{cTr,x}$ is the product of the simulated CC adjusted for micro-advective effects (CC*) and the maximum crop transpiration coefficient ($K_{cTr,x}$). On any day $i$:

$$\text{Tr}_i = K_{s_i} \cdot K_{cTr,x} \cdot CC_i^* \cdot ET_{0_i}. \tag{1}$$

Being a water-driven model, AquaCrop converts Tr directly into $B$ by means of the normalized biomass water productivity (WP) and a cold stress coefficient for biomass production ($K_{s_b}$) in the third step (Eqn 2). WP is the $B$ produced per unit land area and per unit of water transpired, normalized for atmospheric $CO_2$ and for climate.

$$B = \text{WP} \cdot \sum_{i=1}^{n} K_{s_{b_i}} \cdot \frac{\text{Tr}_i}{ET_{0_i}}, \tag{2}$$

where $n$ is the number of sequential days spanning the growing season. Finally, the harvestable fraction of $B$, referred to as $Y$, is determined by means of the harvest index (HI, Eqn 3). While for annual crops, $B$ is referring to the AGB only, ABG + BGB was considered as $B$ for the poplars, and HI was calculated as the fraction of the ABG without the leaves over $B$ (AGB + BGB):

$$Y_i = \text{HI}_i \cdot B_i. \tag{3}$$

The increase in HI over time to reach its final value is described by a logistic function over a specified part of the growing season ($HI_{length}$), starting from an initial HI value ($HI_{ini} = 0.01$) and a HI growth coefficient (HIGC) (Eqn 4):

$$\text{HI}_i = \frac{HI_{ini} \cdot HI}{HI_{ini} + (HI - HI_{ini}) \cdot \exp^{-(\text{HIGC})t}}, \tag{4}$$

where $t$ is the time in days.

During this four-step simulation process, AquaCrop accounts for the effect of various stresses. To account for water stress, AquaCrop determines the SWC in the root zone using a

**Table 2** List of all AquaCrop model parameters with their values for the two calibration years, i.e. the first (R2.1) and the second (R2.2) years of the second rotation

| Parameter | Description | Unit | R2.1 | R2.2 |
|---|---|---|---|---|
| $CC_0$ | Initial green canopy cover | % | 4 | 6 |
| $CC_x$ | Maximum green canopy cover | m² m$^{-2}$ | 0.96 | 0.96 |
| CDC | Canopy decline coefficient | fraction GDD$^{-1}$ | 0.004375 | 0.002302 |
| CGC | Canopy growth coefficient | fraction GDD$^{-1}$ | 0.003131 | 0.004525 |
| Cn | Curve number | | 46 | 46 |
| Eme | Period from sowing to emergence | GDDs | 0 | 0 |
| evardc | Effect of canopy cover in reducing soil evaporation in late season | % | 70 | 70 |
| HI | Harvest index ((AGB-leaves)/$B$) | % | 68 | 68 |
| HIGC | Growth coefficient for HI | day$^{-1}$ | | |
| $HI_{length}$ | Period of harvest index build-up (% of the growing cycle) | % | 50 | 50 |
| $HI_{ini}$ | Initial value for harvest index | % | 0.01 | |
| $K_{c_{Tr,x}}$ | Coefficient of maximum crop transpiration | | 0.99 | 0.99 |
| $K_s$ | Soil water stress coefficient | | 1 | 1 |
| $K_{sat}$ | Saturated hydraulic conductivity | mm day$^{-1}$ | 1200 | 1200 |
| $K_{s_b}$ | Cold stress coefficient | | 1 | 1 |
| Mat | Total length of crop cycle from sowing to maturity | GDDs | 3151 | 3236 |
| mul | Reduction of evaporation by mulches during the growing season | % | 21 | 86 |
| $mul_a$ | Reduction in soil evaporation by mulches after growing season | % | 81 | 81 |
| $mul_b$ | Reduction in soil evaporation by mulches before growing season | % | 63 | 81 |
| Root | Period from sowing to maximum rooting depth | GDDs | 1683 | 1385 |
| rtexlw | Maximum root water extraction in bottom quarter of root zone | m³ m$^{-3}$ soil day$^{-1}$ | 0.009 | 0.009 |
| rtexup | Maximum root water extraction in top quarter of root zone | m³ m$^{-3}$ soil day$^{-1}$ | 0.036 | 0.036 |
| $rt_n$ | Minimum effective rooting depth | m | 0.8 | 0.8 |
| $rt_x$ | Maximum effective rooting depth | m | 0.8 | 0.8 |
| Sen | Period from sowing to start senescence | GDDs | 2482 | 1961 |
| $SWC_{fc}$ | Soil water content at field capacity | vol% | 22 | 22 |
| $SWC_{pwp}$ | Soil water content at wilting point | vol% | 10 | 10 |
| $SWC_{sat}$ | Soil water content at saturation | vol% | 41 | 41 |
| $T_b$ | Base temperature for crop development | °C | 0 | 0 |
| $T_u$ | Upper temperature for crop development | °C | 25 | 25 |
| WP | Water productivity normalized for $ET_0$ and $CO_2$ | g m$^{-2}$ | 10.4 | 14 |

GDDs: growing degree days.

soil water balance that tracks all incoming (rainfall, eventual irrigation, and capillary rise) and outgoing (run-off, deep percolation, soil evaporation [$E_{soil}$], Tr) daily water fluxes. Next to water stress, AquaCrop also considers the effect of temperature, soil salinity, and soil fertility (Van Gaelen et al., 2015). A more detailed description of the AquaCrop model calculation procedures and algorithms has been previously provided (Raes et al., 2009, 2012).

## Model input

AquaCrop (version 5) was run using meteorological data of daily $ET_0$, Pr, minimum temperature ($T_{min}$), and maximum temperature ($T_{max}$). Daily $ET_0$ values were calculated with the FAO Penman–Monteith equation (Allen et al., 1998) based on measured daily $T_{min}$ and $T_{max}$, minimum and maximum RH, $u$ (at 2 m height) and $R_s$.

Soil parameters (Table 2) were estimated based on the site's soil texture. Default values for a loamy sand soil were used to determine the SWC at field capacity ($SWC_{fc}$) and the SWC at

permanent wilting point ($SWC_{pwp}$) as well as for the saturated hydraulic conductivity ($k_{sat}$, Raes, 2015). The SWC at saturation ($SWC_{sat}$) was determined based on SWC observations at those days when the soil was completely saturated because of the shallow SWT. Furthermore, the surface run-off curve number (Cn) was selected based on soil type and forest land use (USDA, 2004), assuming that the initial abstraction equals 5% of surface storage capacity. To consider capillary rise from a shallow SWT, the capillary rise function was calibrated using the default settings for the selected soil texture and $k_{sat}$. The SWT over time and the initial SWC were also entered as input in the model.

## Model calibration and evaluation

Crop parameters of AquaCrop were calibrated based on the observations of the second rotation, i.e. the first multistem rotation of the plantation. The calibration took the different growth strategies (Fig. 1) for the two rotation years into account. After calibration, model simulations of daily SWC, ET, and final $Y$

were validated against field observations of the third rotation (i.e. first 2 years of R3).

Model evaluation, performed for 2.1, R2.2, R3.1, and R.3.2, was based on the graphs of observed and simulated values as well as on the normalized root-mean-square error (NRMSE, normalized over the range of the observed values) and the coefficient of determination ($R^2$). Model performance was considered higher when the NRMSE approached 0 or $R^2$ values approached 1. The reported $P$-values refer to overall $F$-tests, performed to test the hypothesis of a significant linear relationship between observed and simulated values. The model evaluation was carried out, and figures were made with the statistical software R (R 3.2.5, Vienna, Austria. ISBN 3-900051-07-0, URL http://www.R-project.org).

## Results

### Calibration of the model for SRC crop development

The minimum ($rt_n$) and maximum ($rt_x$) effective rooting depth of the crop was based on values of root length published for the study site (Berhongaray *et al.*, 2015), indicating an increasing rooting depth until October of R1.2 and a stable value in R2.1. Therefore, a constant $rt_x$ of 0.8 m was chosen for the simulation period. The timing of crop (leaf) emergence, $CC_x$, the onset of canopy senescence, and the end of the season were all based on LAI measurements. The measured LAI values were converted to CC values (Eqn 5), based on Beer's law of light extinction (Raes, 2015).

$$CC = 1 - \exp(-k \cdot LAI), \tag{5}$$

where $k$ is the light extinction coefficient and $k$ was set to 0.6 for poplar using Eqn 6 (Monsi & Saeki, 1953; Sampson & Allen, 1998; Lunagaria & Shekh, 2006), based on $PAR_t$ and $PAR_i$ measurements in R3.2. This value corresponded to the values reported for poplar (Gielen *et al.*, 2003; Hart *et al.*, 2015; Oliver *et al.*, 2015), although a few lower values had also been observed (Ceulemans *et al.*, 1992).

$$k = \left[ \frac{-\ln(PAR_t/PAR_i)}{LAI} \right]. \tag{6}$$

As stems had to regrow from the coppiced stump, the growing season started later in the first year after the coppice (R2.1) than in the second year of the rotation (R2.2). The timing of crop emergence was 6 April 2012 for R2.1 and 20 March 2013 for R2.2. $CC_0$ also differed with year within the rotation, with 4% cover for R2.1 and 6% cover for R2.2. Given the changing growth strategies in different years (Fig. 1), the CGC and the CDC for plant development were adapted accordingly via calibration based on simulated and observed CC values. The parameters of crop development were initially entered in calendar days (CDs) and subsequently

converted into growing degree days (GDDs) by the model, calculated as $T_{air}$ minus the base temperature for plant development ($T_b$). The validation was then performed using the model based on GDDs.

Depending on the developmental phase of the poplar crop, leaf litter as well as standing vegetation affected the amount of $E_{soil}$. A mulch parameter was included in the model to reduce the evaporation caused by mulches covering the ground. The mulch was composed of organic plant material. Although there was no quantitative measure for the mulching effect, the amount of mulches needed was calibrated by comparing the simulated ET with the observed ET. After coppice, which was carried out in winter (February), only a short woody stump remained of the poplars and the mulching effect was low (Table 2: $mul_b$ for R2.1 = 21%). During the R2.1 growing season, the mulching effect increased to 63% (mul for R2.1), and after the growing season, when the fallen leaves were covering the ground, to 86% ($mul_a$ for R2.1 = $mul_b$ for R2.2). During the R2.2 growing season, the limiting effect on the $E_{soil}$ remained high (mul of 83%), to restore to 86% ($mul_b$ for R2.2) after the growing season until the next coppice.

### Calibration of the model for crop physiology

The $K_{c_{Tr,x}}$ was calculated using eqn (1) based on measured ET and $ET_0$ at mid-season (days on which LAI was between 3.5 and 5), when ET was almost equal to Tr leading to a mean value of 0.99 (90% CI 0.90–1.07). The HI under nonstressed conditions was 68%, with $HI_{ini}$ equal to 0.01% and $HI_{length}$ to 50%. $T_b$ was set to 0 °C (Pellis *et al.*, 2004), and the upper temperature ($T_u$) for optimal development was set to 25 °C. $T_u$ is the upper limit of the optimum temperature range (20–25 °C) for deciduous trees in temperate climate regions (Berry & Björkman, 1980). In modelling studies on SRC optimal temperature, values of 20 and 30 °C were used for, respectively, Canada (Amichev *et al.*, 2010) and the USA (Headlee *et al.*, 2013). Although poplars differ from agricultural crops with respect to habitus, growing cycle, and productivity, the crop parameter ranges were in general applicable to poplars, although some parameters were redundant. Only WP, fine-tuned at the end of the calibration process by comparing the simulated and observed B, was out of the range expected for crops for the first rotation year (10.4 g m$^{-2}$) and on its lower limit for the second rotation year (14 g m$^{-2}$), suggesting a more efficient water use in the second year of R2.

### Environmental conditions

The variable weather conditions during the two rotations led to highly variable atmospheric water demands,

expressed in $ET_0$. In particular, in R3.2, some high peaks in water demand, up to 6.2 mm day$^{-1}$, were observed, coinciding with high ET fluxes (Fig. 2). The calculated annual $ET_0$ value increased during the study period from 592 mm in R2.1 to 862 mm in R3.2. The annual averages of $T_{min}$ and $T_{max}$ were also higher in R3 than

in R2 (Table 3). The annual Pr totals of the 4 years were very similar and ranged between 789 mm and 852 mm (Table 3). Dryer periods coincided with decreasing SWCs. However, the SWC and SWT were primarily affected by the atmospheric and crop water demand leading to the U-shaped curves of daily values (Fig. 2)
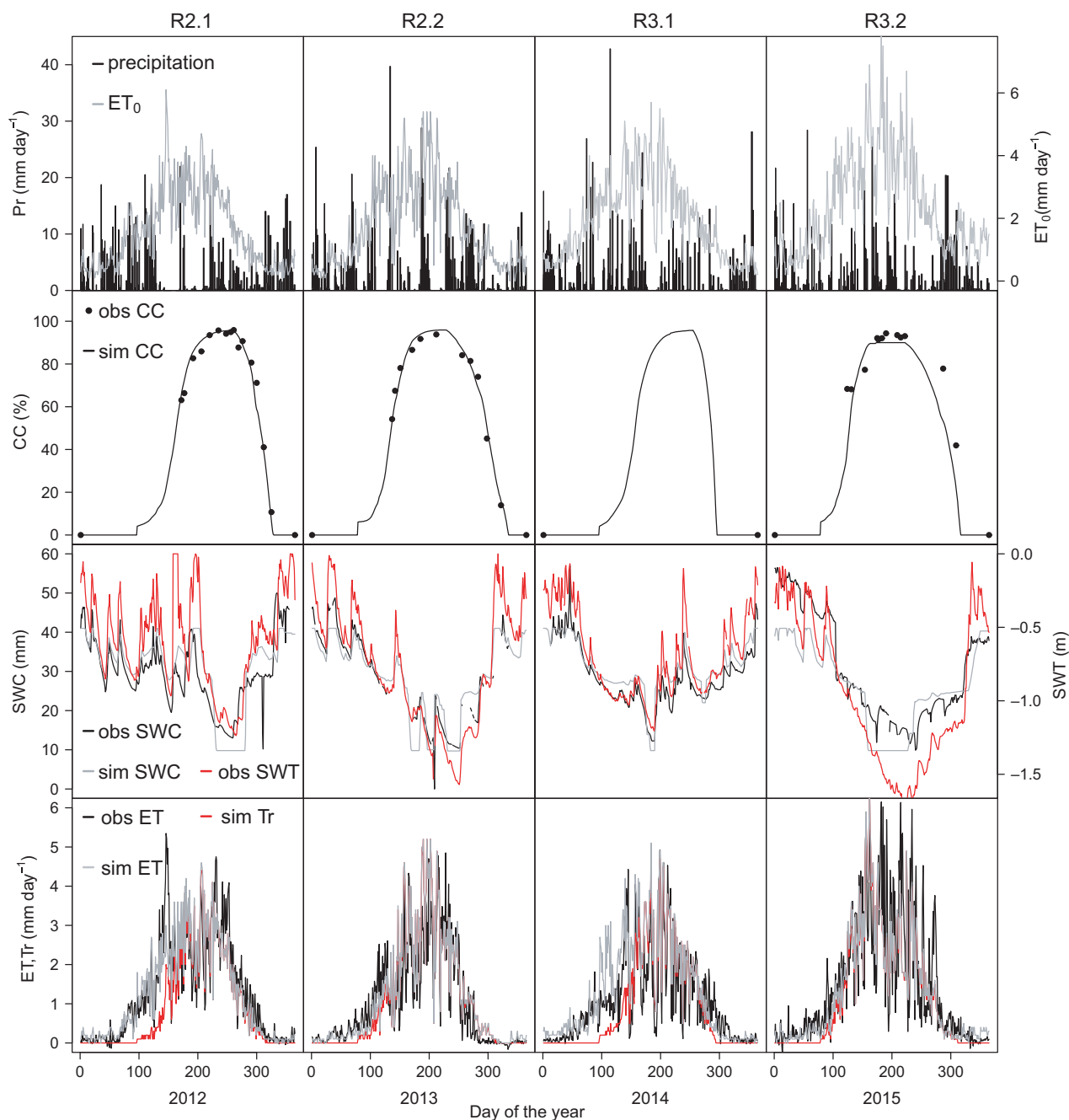


**Fig. 2** Observed (obs) precipitation (Pr) and calculated reference evapotranspiration of a well-watered grassland ($ET_0$) (top panel row); calculated (from leaf area index (LAI) measurements) and simulated (sim) canopy cover (CC) (second panel row); observed and simulated soil water content (SWC) in the upper 0.3 m of the soil and observed soil water table depth (SWT) (third panel row); and observed and simulated evapotranspiration (ET), and simulated transpiration (Tr) (bottom panel row) for R2 and the first 2 years of R3 of the short-rotation coppice plantation. For explanations of R2.1, R2.2, R3.1, and R3.2, see Fig. 1.

in each year. The SWT was generally quite high and reached the deepest level in R3.2, with a maximum depth of 1.72 m on 12 August 2015.

### Simulations of stand water use

Overall, the AquaCrop model showed good performance for the simulation of SWC and of ET (Figs 2 and 3). The largest deviation of simulated SWC from observed SWC occurred during the second half of R2.1 and the first months of R3.2, where SWC was underestimated. The agreements between simulated and observed were excellent in R2.2 and R3.1 with low relative errors (NMRSE values < 10%, $R^2$ = 0.85, $P$ < 0.0001, Table 4), but also the model fits for R2.1 and R3.2 captured a significant part of the total variability in the observed SWC (NRMSE = 16.1 and 17, $R^2$ = 0.57 and 0.76, respectively, $P$ < 0.0001). The strongest deviations from the observations occurred for very low and very high SWC observations.

The observed ET was significantly well fitted by the model ($R^2$ between 0.76 and 0.81, $P$ always <0.0001),

**Table 3** Observed and simulated yearly totals of the reference evapotranspiration calculated for a well-watered grassland ($ET_{0,tot}$), soil evaporation ($E_{soil,tot}$), crop transpiration ($Tr_{tot}$) and evapotranspiration ($ET_{tot}$) daily averages, and maxima of evapotranspiration (ET)

| Variable | R2.1 | R2.2 | R3.1 | R3.2 | Average |
|---|---|---|---|---|---|
| **Observed** | | | | | |
| **Yearly** | | | | | |
| $Pr_{tot}$ (mm) | 788.5 | 851.3 | 852.3 | 804.9 | 824.3 |
| $ET_{tot}$ (mm) | 464.5 | 372.1 | 386 | 536.1 | 439.7 |
| **Daily** | | | | | |
| ET average (mm) | 1.27 | 1.02 | 1.06 | 1.47 | 1.21 |
| ET max (mm) | 5.4 | 4.9 | 4.9 | 6.2 | 5.4 |
| **Simulated** | | | | | |
| **Yearly** | | | | | |
| $ET_{0,tot}$ (mm) | 592 | 636 | 713 | 862 | 701 |
| $E_{soil}$ (mm) | 131 | 29 | 163 | 45 | 92 |
| $Tr_{tot}$ (mm) | 335 | 368 | 328 | 432 | 366 |
| $ET_{tot}$ (mm) | 466 | 398 | 491 | 477 | 458 |
| $ET_{tot}/ET_0$ | 0.85 | 0.62 | 0.69 | 0.55 | 0.68 |
| $Tr_{tot}/ET_{tot}$ | 0.72 | 0.93 | 0.67 | 0.81 | 0.78 |
| $E_{soil,tot}/ET_{tot}$ | 0.28 | 0.07 | 0.33 | 0.19 | 0.22 |
| **Daily** | | | | | |
| ET average (mm) | 1.27 | 1.17 | 1.34 | 1.32 | 1.28 |
| ET max (mm) | 4.6 | 5.2 | 5.1 | 6.5 | 5.4 |

For the observations, the total precipitation ($Pr_{tot}$) and the average daily minimum ($T_{min}$) and maximum ($T_{max}$) temperatures are given. For the simulations, the fractions of ET over $ET_0$, of $E_{soil}$ over ET, and of Tr over ET are also shown. For explanations of R2.1, R2.2, R3.1, and R3.2, see Fig. 1.

with NRMSE values between 10% and 15% for all years. However, the simulated ET seemed to miss extreme peaks in observed ET values. The latter was especially true at the onset of the growing season R2.1, and from June till the end of the season in R3.2. The smoothed splines of simulated and observed daily ET values showed that the maximum ET was overestimated in all years and that, for some years, ET raised too fast in the beginning of the season. The simulation results therefore often exceeded the random uncertainty boundaries of the EC measurements between May and August (Fig. 4). Longer periods of overestimated ET values were observed for R2.2 and R3.1. In R3.2, there was a steep decline in simulated ET in June, when SWT started to drop, which caused an underestimation of ET during the summer.

The total annual ET ($ET_{tot}$) of the SRC was lower than the total annual $ET_0$ ($ET_{0,tot}$), especially in the second year of both rotations (Table 3) where the fractions of simulated $ET_{tot}$ over $ET_{0,tot}$ were only 0.62 (for R2.2) and 0.55 (for R3.2). For the first year of both rotations, these fractions were higher with values of 0.85 (R2.1) and 0.69 (R3.1). The fraction of the simulated yearly Tr ($Tr_{tot}$) over the simulated $ET_{tot}$ was higher in the second years (>0.8) than in the first years of both rotations (0.72 vs. 0.67). Daily averages of simulated ET in the different years were similar. The average of the simulated daily ET over the 4 years was 1.3 mm day$^{-1}$. For the observed ET, this average value was 1.2 mm day$^{-1}$. The maxima of daily ET ranged from 4.6 to 6.5 mm day$^{-1}$ for the simulations and from 4.9 to 6.2 mm day$^{-1}$ for the observations. The overall maximum daily ET averaged over the 4 years of the study, 5.4 mm day$^{-1}$, was identical for the simulations and the observations (Table 3).

The energy balance closure at the site ranged from 65% to 81% of the total available energy (Fig. 5) depending on the year and on the time in the growing season. The linear regressions between the available energy and the measured energy fluxes were all highly significant ($P$ < 0.0001).

### Simulations of crop development and yield

Relative errors of the CC fits were low (NRMSE < 10%), and the fit was highly significant for the calibration years ($R^2$ = 97%, $P$ < 0.0001 for both calibration years) and for the validation year R3.2. (NRMSE = 12.9%; $R^2$ = 93%, $P$ < 0.0001; Table 4). Crop development differed depending on the year with an earlier start of the leaf area development in the noncoppice years (Broeckx *et al.*, 2015; Vanbeveren *et al.*, 2016a). In the model, the growing season started 18 CDs (or 298 GDDs) later for the first year than for the second year of each rotation,

but in both rotation years, the same $CC_x$ of 96% was reached. The CC increased somewhat faster when no coppice was executed during the winter before. The total length of the growing season counted 3151 GDDs for R2.1 and 3236 GDDs for R2.2 (Table 2).

The observed (calculated from the measured AGB and BGB) and simulated $B$ were, respectively, 21.73 and 22.12 Mg ha$^{-1}$ yr$^{-1}$ for R2.1 vs. 15.11 and 15.01 Mg ha$^{-1}$ yr$^{-1}$ for R2.2. The observed $Y$ was markedly higher for the calibration period (R2) than for the validation period (R3), with a decrease of 35.6% for R3.1 compared to R2.1, and of 30.6% for R3.2 compared to R2.2 (Fig. 1, Table 5). $Y$ was simulated well for the calibration years, with less than 1% discrepancy. In contrast, $Y$ was overestimated for both validation years, with deviations from the observed values of 32.2% for R3.1 and of 33.6% for R3.2 (Table 5).

## Discussion

In this study, the potential of the AquaCrop model to simulate the water use and the $Y$ of SRCs was examined. Based on data from the second and the third rotation of a rainfed poplar SRC, the results evidenced the
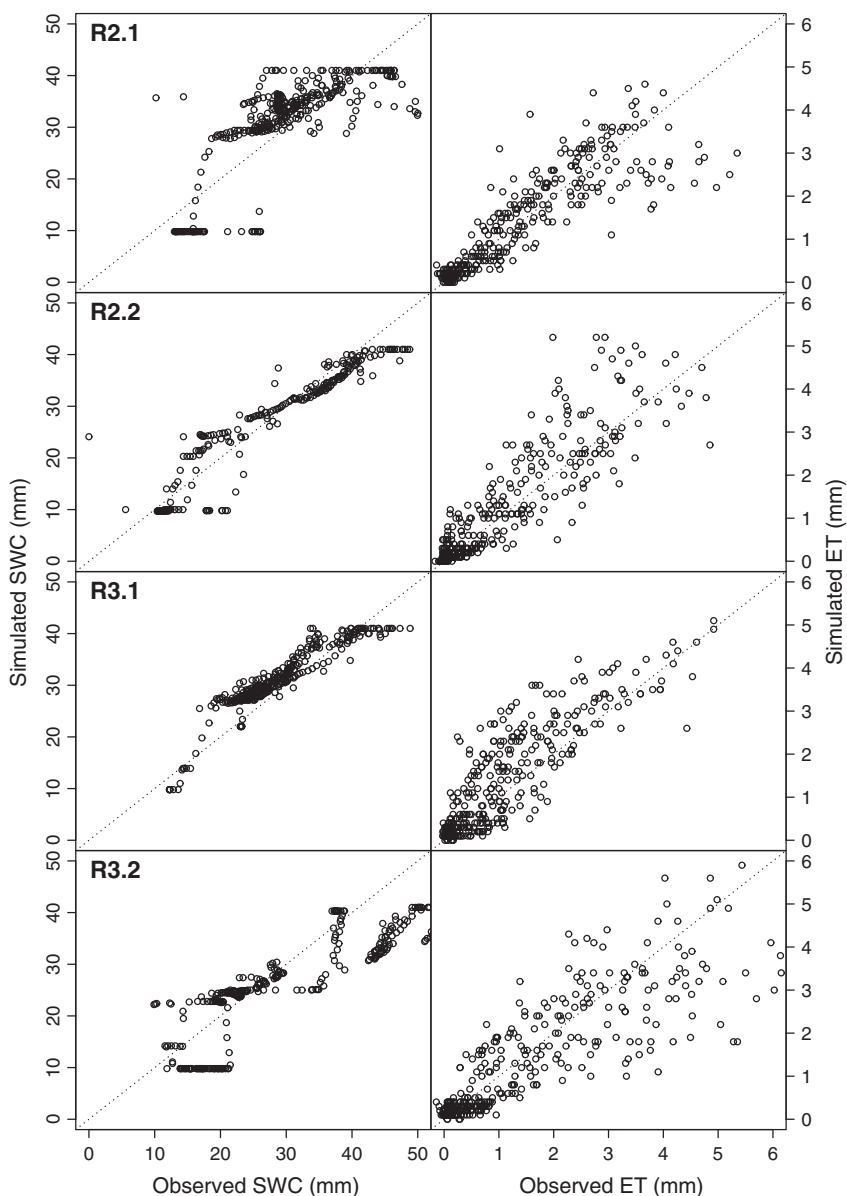


**Fig. 3** Simulated values of the daily soil water content (SWC) and evapotranspiration (ET) against observed values for all years. For explanations of R2.1, R2.2, R3.1, and R3.2, see Fig. 1. Grey, dotted lines show the 1 : 1 line.

**Table 4** Number of observations ($n$), R-square ($R^2$), and normalized root-mean-square error (NRMSE, in %) values for the daily soil water content (SWC) in the upper 0.3 m of the soil, for daily evapotranspiration (ET), and for canopy cover (CC) simulations. For explanations of R2.1, R2.2, R3.1, and R3.2, see Fig. 1.

| Variable | Statistic | R2.1 | R2.2 | R3.1 | R3.2 |
|---|---|---|---|---|---|
| SWC | $n$ | 355 | 231 | 351 | 360 |
| | $R^2$ | 0.57 | 0.85 | 0.85 | 0.76 |
| | NRMSE | 16.1 | 9.4 | 8.1 | 17.0 |
| ET | $n$ | 365 | 365 | 365 | 365 |
| | $R^2$ | 0.78 | 0.81 | 0.76 | 0.76 |
| | NRMSE | 10.8 | 10.9 | 13.6 | 12 |
| CC | $n$ | 15 | 11 | | 11 |
| | $R^2$ | 0.97 | 0.97 | | 0.87 |
| | NRMSE | 5.0 | 4.6 | | 12.9 |

accurate simulation of ET and Tr by AquaCrop as well as the model's capacity to predict the potential $Y$ of SRCs. The yield gap could, at least partly, be explained by the occurrence of an extensive weedy understory layer.

*Simulations of stand water use*

The observed and simulated $ET_{tot}$ values were comparable to the $ET_{tot}$ values between 241 and 520 mm reported for extensively managed SRC plantations in Europe (a.o. Schmidt-Walter *et al.*, 2014; Zenone *et al.*, 2015; Bloemen *et al.*, 2016). The $K_{cTr,x}$ value for the calibration period (0.99) was compared well with the values published for the Czech Republic (0.92; Fischer *et al.*, 2013) and for Germany (0.94; Schmidt-Walter *et al.*, 2014), and was within the range of the values of a comparative literature survey (cfr. table 5 in Fischer *et al.*, 2013). Much higher $ET_{tot}$ and $K_{cTr,x}$ values were reported for well-irrigated sites with values up to 1100 mm for $ET_{tot}$ and of 4.28 for $K_{cTr,x}$ in combination with fertilization (Deckmyn *et al.*, 2004; Guidi *et al.*, 2008; Pistocchi *et al.*, 2009). However, high water demands have also been measured on poplars for some unirrigated sites in Europe (Allen *et al.*, 1999; Meiresonne *et al.*, 1999; Hall, 2003).

Our $Tr_{tot}/ET_{tot}$ values were in line with the average value of 0.75 published in a review article using 271
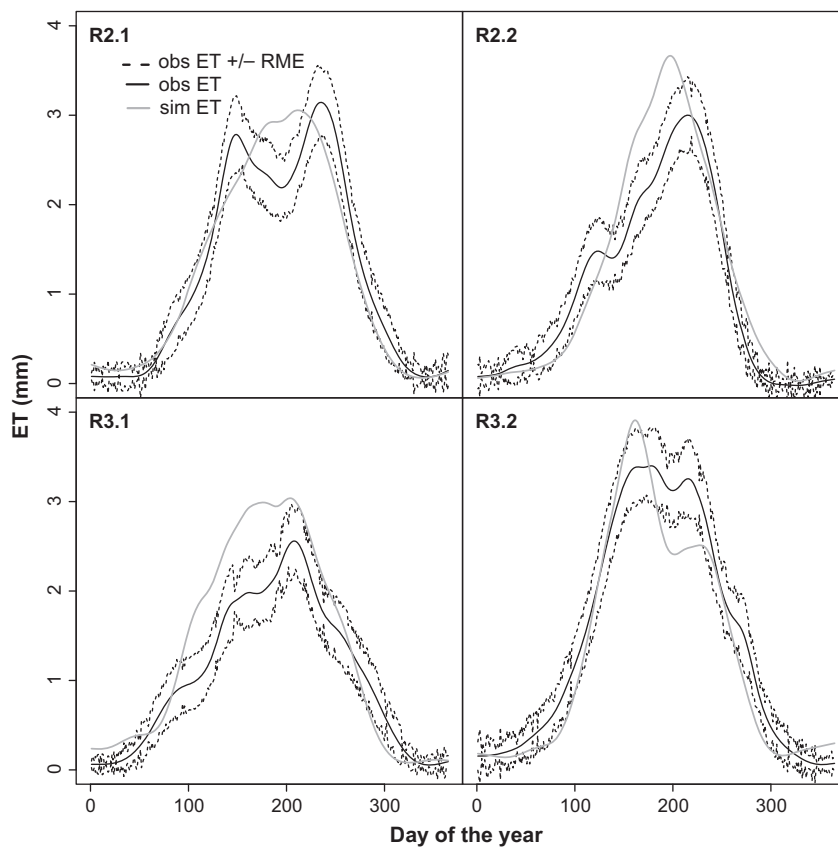


**Fig. 4** Smoothed spline curves of observed (obs) daily evapotranspiration (ET) values with the (unsmoothed) daily random measurement error (RME), and the smoothed simulated (sim) daily ET values for the 2 years of R2 and the first 2 years of R3. For explanations of R2.1, R2.2, R3.1 and R3.2, see Fig. 1.
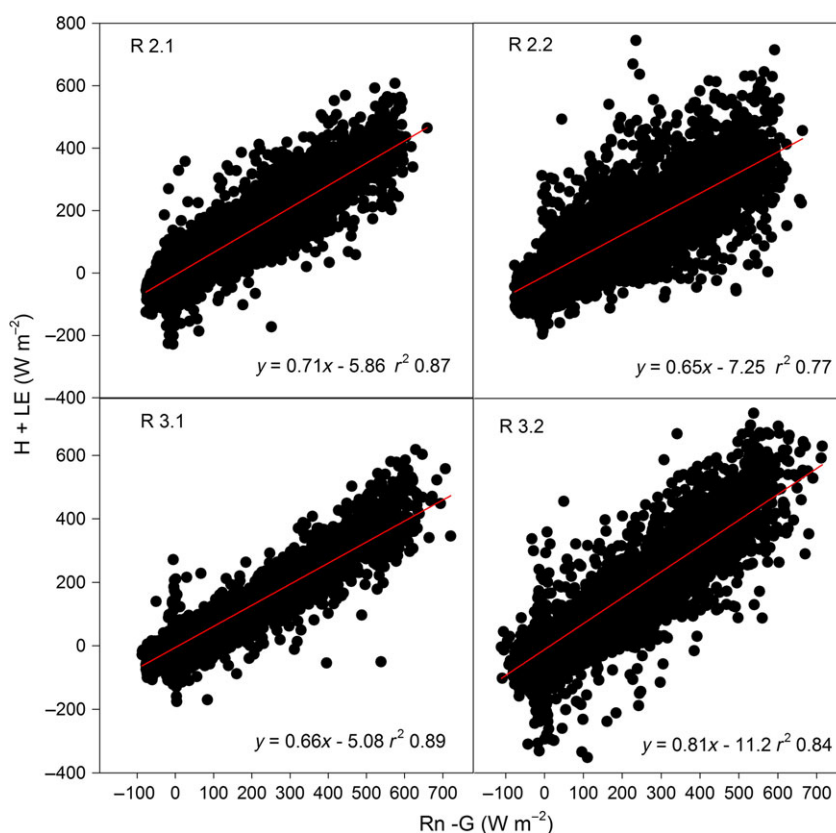
**Fig. 5** Energy balance closure for the 4 years of the study. Red lines are the linear regression lines. The regression equation between measured energy fluxes and available energy is also presented. For explanations of R2.1, R2.2, R3.1, and R3.2, see Fig. 1.

**Table 5** Observed vs. simulated yield (Mg ha$^{-1}$ yr$^{-1}$), together with the deviation of the simulated values from the observed values

| Year | Observed yield | Simulated yield | Deviation | Relative deviation (%) |
|------|------|------|------|------|
| R2.1 | 10.26 | 10.20 | −0.06 | −0.58 |
| R2.2 | 14.76 | 14.63 | −0.13 | −0.88 |
| R3.1 | 6.61 | 8.74 | 2.13 | 32.22 |
| R3.2 | 10.25 | 13.69 | 3.44 | 33.56 |

Negative deviation: underestimation; positive deviation: overestimation of the yield. For explanations of R2.1, R2.2, R3.1, and R3.2, see Fig. 1.

studies on nonfood woody tree plantations (King *et al.*, 2013). The fractions were lower for the second years of each rotation when the soil was covered by more standing biomass in the beginning and by more mulch after the growing season (i.e. standing woody biomass and litter). In the beginning of the growing season, more leaf area was transpiring and the resistance for $E_{soil}$ was higher. The yearly averages of simulated Tr values were higher than the values from 0.36 to 0.88 mm day$^{-1}$

simulated for the UK with the JULES land-surface model (Oliver *et al.*, 2015). The logarithmic relation between CC and LAI could possibly cause an overestimation of Tr at medium LAI values, when CC had reached its maximum. Another possible difficulty in the simulation of Tr during the growing season is the changing surface conductance of the crop during canopy development (Zenone *et al.*, 2015). Finally, the radiation regime and cooler climatic conditions might also explain our higher Tr values.

Difficulties inherent to the use of the SWC sensors might have been the cause of the unrealistically high values of SWC in the original data set. At the start of R3.2, the SWC and SWT sensors were changed, resulting in a strong but temporary bias in that year. One reason for the dissimilarities in the SWC simulations at high observed SWCs is that we limited the SWC to a value of 41% during model calibration.

*Simulations of canopy development and yield*

AquaCrop was able to simulate the effect of coppice on the canopy development using two sets of parameters,

one for each year of the rotation cycle. The second growing season of the rotation was set to start later compared to the first, as was derived from the LAI data, but also shown by the use of Webcam and MODIS data on the same plantation during R1.2 and R2.1 (Vanbeveren *et al.*, 2016a). Developments of the AquaCrop software, as to deal with changing crop characteristics of perennial crops, are in progress.

Our observed and simulated $Y$ values were well within the range observed and simulated for SRC plantations in the UK (between 5.1 and 16.2 Mg ha$^{-1}$ yr$^{-1}$; Tallis *et al.*, 2013; Oliver *et al.*, 2015) and in north-central USA (between 4.4 and 13 Mg ha$^{-1}$ yr$^{-1}$; Headlee *et al.*, 2013).

The overestimation of $Y$ in both validation years suggests a yield gap in R3. One possible explanation for the 30% yield gap could be the high relative leaf cover of weeds (RC) in R3. The weed infestation became larger in each subsequent rotation and decreased because of light competition over the years within each rotation (direct observations by field technicians), reaching an average RC value of 22% of the total vegetation in R3.3 (assessed by careful inspection of each genotypic block by seven persons on 15 July 2016). For R3.1 and R3.2, the RC was thus larger than 22% and larger than the RC in R2. Weeds grew up to 1.5 m height and accumulated up to 300 g C m$^{-2}$ in biomass (Berhongaray & Ceulemans, 2015; Berhongaray *et al.*, 2015) and the weed root biomass reached more than two times the fine root biomass of the poplars already in the first rotation (Berhongaray *et al.*, 2013). A technical release of a future version of the AquaCrop model including a weed module (Van Gaelen *et al.*, 2016) resulted in a correct estimation of the yield (10.22 Mg ha$^{-1}$ yr$^{-1}$) in R3.2 when an RC of 27% was used. Weakening vitality might also be an explanation for the yield gap (Geyer, 2006). At our site, 15% cutting mortality was observed after R1.1, i.e. during the establishment year (Verlinden *et al.*, 2015). Thereafter, mortality remained nearly unchanged until the end of R2 and increased by 5% in R3 (Stefan Vanbeveren, nonpublished data). Nutrient availability did not decrease since the start of the plantation in 2010 (Vanbeveren *et al.*, 2016b). However, management (irrigation, rotation length, fertilization, herbicide and pesticide application, harvesting, clone selection) and nutrient availability have interactive effects on the $Y$ of SRC plantations (Sabatti *et al.*, 2014). The rather low WP values compared to annual crops (Raes *et al.*, 2012) might be due to the relatively high energy cost for lignin production, and hence the enhanced respiration for the wood formation.

## Uncertainties

The model output was restricted by the uncertainties on both the observed and the simulated data. For example, ET observations from EC measurements rely on assumptions during their calculation (Rebmann *et al.*, 2012). Furthermore, the lack of energy balance closure in the EC data could cause an underestimation of the ET values (Zona *et al.*, 2013; Zenone *et al.*, 2015). The model simulations were also prone to uncertainty concerning robustness of the parameters and model structure. Although the simplified and water-driven structure of the model was effective, the multilayered vegetation structure of perennial trees, even if intensively managed, is more complicated than that of an annual crop. In the process-based radiation or leaf area-driven yield models, LAI is a crucial variable (Martin & Jokela, 2004; Fabrika & Pretzsch, 2013; Waring *et al.*, 2016). When using the AquaCrop model, data of CC on experimental sites are required to check the influence of the LAI to CC conversion on the simulated ET and consequently also on $Y$. Different techniques, e.g. line intersect sampling, spherical densiometer and digital or satellite imaging, are available to measure the canopy development (Korhonen *et al.*, 2006; Vanbeveren *et al.*, 2016a). The uncertainties on the model simulations were not considered in this study, but global (Vanuytrecht *et al.*, 2014a) and specific (one by one for the most influential parameters) sensitivity analyses (Bloemen *et al.*, 2016) of AquaCrop were already performed.

In conclusion, this study demonstrated that the agricultural AquaCrop model enabled to simulate canopy water consumption of a fast-growing SRC crop in a very reliable way, even if the model's concepts and calculation procedures were originally tailored to annual crops. The model also simulated the gap between potential and realized yield caused by problems in the actual management, by the environment or by dominating RC amounts.

## References

Adler PR, Del Grosso SJ, Patron WJ (2007) Life-cycle assessment of net greenhouse-gas flux for bioenergy cropping systems. *Ecological Applications*, **17**, 675–691.

AEBIOM (2012) *European bioenergy outlook.* Statistical Report, European Biomass Association, Brussels, 123 pp.

Allen RG, Pereira LS, Raes D, Smith M (1998) *Crop evapotranspiration: guidelines for computing crop water requirements. FAO Irrigation and drainage paper No. 56.* FAO, Rome, Italy.

Allen SJ, Hall RL, Rosier PTW (1999) Transpiration by two poplar varieties grown as coppice for biomass production. *Tree Physiology*, **19**, 493–501.

Amichev BY, Johnston M, Van Rees KCJ (2010) Hybrid poplar growth in bioenergy production systems: biomass prediction with a simple process-based model (3PG). *Biomass and Bioenergy*, **34**, 687–702.

Ayllot JA, Casella E, Tubby I, Street NR, Smith P, Taylor G (2008) Yield and spatial supply of bioenergy poplar and willow short-rotation coppice in the UK. *New Phytologist*, **178**, 358–370.

Baum C, Leinweber P, Weih M, Lamersdorf N, Dimitriou I (2009) Effects of short rotation coppice with willows and poplars on soil ecology. *Agriculture and Forestry Research*, **3**, 183–196.

Berhongaray G, Ceulemans R (2015) Neglected carbon pools and fluxes in the soil balance of short-rotation woody biomass crops. *Biomass and Bioenergy*, **73**, 62–66.

Berhongaray G, Janssens IA, King JS, Ceulemans R (2013) Fine root biomass and turnover of two fast-growing poplar genotypes in a short-rotation coppice culture. *Plant and Soil*, **373**, 269–283.

Berhongaray G, Verlinden MS, Broeckx LS, Ceulemans R (2015) Changes in below-ground biomass after coppice in two *Populus* genotypes. *Forest Ecology and Management*, **337**, 1–10.

Berhongaray G, Verlinden MS, Broeckx LS, Janssens IA, Ceulemans R (2016) Soil carbon and belowground carbon balance of a short-rotation coppice: assessment from three different approaches. *Global Change Biology Bioenergy*, **9**, 299–313.

Berry J, Björkman O (1980) Photosynthetic response and adaptation to temperature in higher plants. *Annual Review of Plant Physiology*, **31**, 491–543.

Bloemen J, Fichot R, Horemans JA, Broeckx LS, Verlinden MS, Zenone T, Ceulemans R (2016) Water use of a multigenotype poplar short rotation coppice from tree to stand scale. *Global Change Biology Bioenergy*, **9**, 370–384.

Boehmel C, Lewandowski I, Claupein W (2008) Comparing annual and perennial energy cropping systems with different management intensities. *Agricultural Systems*, **96**, 224–236.

Broeckx LS, Verlinden MS, Ceulemans R (2012) Establishment and two-year growth of a bio-energy plantation with fast-growing *Populus* trees in Flanders (Belgium): effects of genotype and former land use. *Biomass and Bioenergy*, **42**, 151–163.

Broeckx LS, Vanbeveren SP, Verlinden MS, Ceulemans R (2015) First vs. second rotation of a poplar short rotation coppice: leaf area development, light interception and radiation use efficiency. *IForest – Biogeosciences and Forestry*, **8**, 565–573.

Ceulemans R (1996) An inventory of tree and stand growth models with potential application in short-rotation forestry. *Biomass and Bioenergy*, **11**, 95–107.

Ceulemans R, Deraedt W (1999) Production physiology and growth potential of poplar under short-rotation forestry culture. *Forest Ecology and Management*, **121**, 9–23.

Ceulemans R, Impens I, Mau F, Van Hecke P, Chen SG (1992) Dry mass production and solar radiation conversion efficiency of poplar clones. In: *Biomass for Energy, Industry and Environment* (eds Grassi , G , Collina A, Zibetta H), pp. 157–163. Elsevier Applied Science, Elsevier Science Publisher Ltd, Barking, UK.

Deckmyn G, Laureysens I, Garcia J, Muys B, Ceulemans R (2004) Poplar growth and yield in short rotation coppice: model simulations using the process model SECRETS. *Biomass and Bioenergy*, **25**, 221–227.

Dillen SY, Rood SB, Ceulemans R (2010) Growth and physiology. In: *Plant Genetics and Genomics Volume 8: Genetics and Genomics of Populus* (eds Jansson S, Bhalerao S, Groover A), pp. 39–63. Springer Science + Business Media, New York.

Dimitriou I, Busch G, Jacobs G, Schmidt-Walter P, Lamersdorf N (2009) A review of the impacts of short rotation coppice cultivation on water issues. *Agriculture and Forestry Research*, **3**, 197–206.

Don A, Osborne B, Hastings A *et al.* (2011) Land use change to bioenergy production in Europe: implications for the greenhouse gas balance and soil carbon. *Global Change Biology Bioenergy*, **4**, 372–391.

Elbehri A, Azapagic A, Cheserek B *et al.* (2015) *Kenya's tea sector under climate change: an impact assessment and formulation of a climate smart strategy.* FAO report. FAO, Rome, Italy. 165 pp.

Fabrika M, Pretzsch H (2013) Chapter 8: Methods of process modelling of forest ecosystems. In: *Forest Ecosystem Analysis and Modelling*, pp. 415–468. Technical University in Zvolen, Bratislava, Slovakia.

Fischer M, Trnka M, Kucera J *et al.* (2013) Evapotranspiration of a high-density poplar stand in comparison with a reference grass cover in the Czech-Moravian highlands. *Agricultural and Forest Meteorology*, **181**, 43–60.

Fischer M, Fichot R, Albaugh JM, Ceulemans R, Domec JC, Trnka M, King JS (2015) *Populus and Salix* grown in a short-rotation coppice for bioenergy: Ecophysiology, aboveground productivity, and stand-level water use efficiency. In: *Sustainable Biofuels, An Ecological Assessment of the Future Energy* (eds Bhardwaj Ajay K, Zenone T, Chen J), pp. 155–194. HEP de Gruyter, Berlin.

Foken T (2008) The energy balance closure problem: an overview. *Ecological Applications*, **18**, 1351–1367.

Geyer WA (2006) Biomass production in the Central Great Plains USA under various coppice regimes. *Biomass and Bioenergy*, **30**, 778–783.

Gielen B, Liberloo M, Bogaert J *et al.* (2003) Three years of free-air $CO_2$ enrichment (POPFACE) only slightly affect profiles of light and leaf characteristics in closed canopies of *Populus*. *Global Change Biology*, **9**, 1022–1037.

Guidi W, Piccioni E, Bonari E (2008) Evapotranspiration and crop coefficient of poplar and willow short-rotation coppice used as vegetation filter. *Bioresource Technology*, **99**, 4832–4840.

Hall RL (2003) *Short rotation coppice for energy production hydrological guidelines.* B/CR/00783/GUIDELINES/SRC, URN03/883, DTI New and Renewable Energy Programme, Bristol, UK, 21 pp.

Hart QJ, Tittmann PW, Bandaru V, Jenkins BM (2015) Modelling poplar growth as a short rotation woody crop for biofuels in the Pacific Northwest. *Biomass and Bioenergy*, **79**, 12–17.

Headlee LW, Zalesny Jr RS, Donner DM, Hall RB (2013) Using a process-based model (3-PG) to predict and map hybrid poplar productivity in Minnesota and Wisconsin, USA. *Bioenergy Research*, **6**, 196–210.

Hollinger DY, Richardson AD (2005) Uncertainty in eddy covariance measurements and its application to physiological models. *Tree Physiology*, **25**, 873–885.

Kim D, Kaluarachchi J (2015) Validating FAO AquaCrop using Landsat images and regional crop information. *Agricultural Water Management*, **149**, 143–155.

King JS, Ceulemans R, Albaugh JM *et al.* (2013) The challenges of lignocellulosic bioenergy in a water-limited world. *BioScience*, **63**, 102–117.

Kollas C, Lasch P, Rock J, Suckow F (2009) Bioenergy potential in Germany – assessing spatial patterns of biomass production with aspen short-rotation coppice. *International Agrophysics*, **23**, 343–352.

Korhonen L, Korhonen KT, Rauiainen M, Stenberg P (2006) Estimation of forest canopy cover: a comparison of field measurement techniques. *Silva Fennica*, **4**, 577–588.

Korzukhin D, Ter-Mikaelian M, Wagner G (1996) Process versus empirical models: which approach for forest ecosystem management? *Canadian Journal of Forest Research*, **26**, 879–887.

Larocque GR, Bhatti J, Arsenault A (2014) Integrated modelling software platform development for effective use of ecosystem models. *Ecological Modelling*, **288**, 195–202.

Lasslop G, Reihstein M, Papale D *et al.* (2010) Separation of net ecosystem exchange into assimilation and respiration using a light response curve approach: critical issues and global evaluation. *Global Change Biology*, **16**, 187–208.

Ledin S, Willebrand A (1996) *Handbook on how to grow short rotation forests.* Technical report, Swedish University of Agricultural Sciences, Uppsala, Sweden, 330 pp.

Lunagaria MM, Shekh AM (2006) Radiation interception, light extinction coefficient and leaf area index of wheat (*Triticum aestivum* L.) crop as influenced by row orientation and row spacing. *The Journal of Agricultural Sciences*, **2**, 43–54.

Martin TA, Jokela EJ (2004) Stand development and production dynamics of loblolly pine under a range of cultural treatments in north-central Florida USA. *Forest Ecology and Management*, **192**, 39–58.

Matala J, Hynynen J, Miina J *et al.* (2003) Comparison of a physiological model and a statistical model for prediction of growth and yield in boreal forests. *Ecological Modelling*, **161**, 95–116.

Meiresonne L, Nadezhdina N, Cermak J, Van Slycken J, Ceulemans R (1999) Measured sap flow and simulated transpiration from a poplar stand in Flanders (Belgium). *Agricultural and Forest Meteorology*, **96**, 165–179.

Mohren GMJ, Burkhart HE (1994) Contrasts between biologically-based process models and management – oriented growth and yield models. *Forest Ecology and Management*, **69**, 1–5.

Monsi M, Saeki T (1953) Über den Lichtfaktor in den Pflanzengesellschaften und seine Bedeutung für die Stoffproduktion. *Japanese Journal of Botany*, **14**, 22–52.

Njakou Djomo S, El Kasmioui O, Ceulemans R (2011) Energy and greenhouse gas balance of bioenergy production from poplar and willow: a review. *Global Change Biology Bioenergy*, **3**, 181–197.

Njakou Domo S, El Kasmioui O, De Groote T *et al.* (2013) Energy and climate benefits of bioelectricity from low-input short rotation woody crops on agricultural land over a two-year rotation. *Applied Energy*, **111**, 1–9.

Oliver RJ, Blyth E, Taylor G, Finch JW (2015) Water use and yield of bioenergy poplar in future climates: modelling the interactive effects of elevated atmospheric $CO_2$ and climate on productivity and water use. *Global Change Biology Bioenergy*, **7**, 958–973.

Pellis A, Laureysens I, Ceulemans R (2004) Genetic variation of the bud and leaf phenology of seventeen poplar clones in a short rotation coppice culture. *Plant Biology*, **6**, 38–46.

Perry CH, Miller RC, Brooks KN (2001) Impacts of short-rotation hybrid poplar plantations on regional water yield. *Forest Ecology and Management*, **143**, 143–151.

Petzold R, Schwärzel K, Feger KH (2010) Transpiration of a hybrid plantation in Saxony (Germany) in response to climate and soil conditions. *European Journal of Forest Research*, **130**, 695–706.

Pistocchi C, Guidi W, Piccioni E, Bonari E (2009) Water requirements of poplar and willow vegetation filters grown in lysimeter under Mediterranean conditions: results of the second rotation. *Desalination*, **246**, 137–146.

Raes D (2015) *AquaCrop Training Handbook. Book I: Understanding AquaCrop*, Chapter 3, p. 11–17. FAO, Rome, Italy.

Raes D, Steduto P, Hsiao C, Fereres E (2009) AquaCrop – the FAO crop model to simulate yield responses to water: II. Main algorithms and software description. *Agronomy Journal*, **101**, 438–447.

Raes D, Steduto P, Hsiao TC, Fereres E (2012) *AquaCrop Reference manual (Version 4.0)*, Chapter 3. FAO, Rome, Italy.

Rallo G, Agnese C, Minacapilli M, Provenzano G (2012) Assessing AquaCrop water stress function to evaluate the transpiration reductions of olive mature trees. *Italian Journal of Agrometeorology*, **1**, 21–28.

Rebmann C, Kolle O, Heainesch B, Quick R, Ibrom A, Aubinet M (2012) Data acquisition and flux calculations. In: *Eddy Covariance, A Practical Guide to Measurements and Data Analysis* (eds Aubinet M, Vesala T, Papale D), pp. 59–84. Springer Atmospheric Sciences, Dordrecht, the Netherlands.

Reichstein M, Falge E, Baldocchi D et al. (2005) On the separation of net ecosystem exchange into assimilation and ecosystem respiration: review and improved algorithm. *Global Change Biology*, **11**, 1424–1439.

Sabatti M, Fabbrini F, Harfouche A, et al. Evaluation of biomass potential and heating value of hybrid popular genotypes in a short-rotation culture in Italy. *Industrial Crops and Products*, **61**, 62–73.

Sampson DA, Allen HL (1998) Light attenuation in a 14-year-old loblolly pine stand as influenced by fertilization and irrigation. *Trees*, **13**, 80–87.

Sands PJ, Battaglia M, Mummery D (2000) Application of process-based models to forest management: experience with PROMOD, a simple plantation productivity model. *Tree Physiology*, **20**, 383–392.

Schmidt-Walter PS, Richter F, Herbst M, Schuldt B, Lamersdorf NP (2014) Transpiration and water use strategies of a young and full-grown short rotation coppice differing in canopy cover and leaf area. *Agricultural and Forest Meteorology*, **195–196**, 165–178.

Segerstedt A, Bobert J (2013) Revising the potential of large-scale *Jatropha* oil production in Tanzania: an economic land evaluation assessment. *Energy Policy*, **57**, 491–505.

Steduto P, Hsiao TC, Raes D, Fereres E (2009) AquaCrop – the FAO crop model to simulate yield response to water: I. Concepts and underlying principles. *Agronomy Journal*, **101**, 426–437.

Tallis MJ, Casella E, Henshall PA, Aylott MJ, Randle TJ, Morison JIL, Tayor G (2013) Development and evaluation of ForestGrowth-SRC a process-based model for short rotation coppice yield and spatial supply reveals poplar uses water more efficiently than willow. *Global Change Biology Bioenergy*, **5**, 53–66.

USDA (2004) Estimation of direct runoff from storm rainfall. In: *Part 630 Hydrology, National Engineering Handbook*, Chapter 10. Natural Resources Conservation Service, Washington, DC, USA. Available at: https://directives.sc.egov.usda.gov/OpenNonWebContent.aspx?content=17752.wba (accessed 31 December 2016)

Van Gaelen H, Tsegay A, Delbecque N et al. (2015) A semi-quantitative approach for modelling crop response to soil fertility: evaluation of the AquaCrop procedure. *Journal of Agricultural Science*, **153**, 1218–1233.

Van Gaelen H, Delbecque N, Abrha B, Tsegay A, Raes D (2016) Simulation of crop water productivity in weed-infested fields for data-scarce regions. *Journal of Agricultural Science*, **154**, 1026–1039.

Vanbeveren SPP, Bloemen J, Balzarolo M, Broeckx S, Sarzi-Falchi I, Verlinden MS, Ceulemans R (2016a) A comparative study of four approaches to assess phenology of *Populus* in a short-rotation coppice culture. *IForest – Biogeosciences and Forestry*, **9**, 682–689.

Vanbeveren SPP, Gebauer R, Plichta R, Volarik D, Ceulemans R (2016b) Nutrients and energy in proleptic branches and leaves of poplar under a short-rotation coppice. *Biomass and Bioenergy*, **85**, 271–277.

Vanuytrecht E, Raes D, Willems P (2014a) Global sensitivity analysis of yield output from the water productivity model. *Environmental Modelling & Software*, **51**, 323–332.

Vanuytrecht E, Raes D, Steduto P et al. (2014b) AquaCrop: FAO's crop water productivity and yield response model. *Environmental Modelling & Software*, **62**, 351–360.

Verheyen K, Buggenhout M, Vangansbeke P, De Dobbelaere A, Verdonckt P, Bonte D (2014) Potential of short rotation coppice plantations to reinforce functional biodiversity in agricultural landscapes. *Biomass and Bioenergy*, **67**, 435–442.

Verlinden MS, Broeckx LS, Van den Bulcke J, Van Acker J, Ceulemans R (2013) Comparative study of biomass determinants of 12 poplar (*Populus*) genotypes in a high-density short-rotation culture. *Forest Ecology and Management*, **307**, 101–111.

Verlinden MS, Broeckx LS, Ceulemans R (2015) First vs. second rotation of a poplar short rotation coppice: above-ground biomass productivity and dynamics. *Biomass and Bioenergy*, **73**, 174–185.

Waring R, Landsberg J, Linder S (2016) Tamm review: insights gained from light use and leaf growth efficiency indices. *Forest Ecology and Management*, **379**, 232–242.

Wohlfahrt G, Irschick C, Thalinger B, Hörtnagl L, Obojes N, Hammerle A (2010) Insights from independent evapotranspiration estimates for closing the energy balance: a grassland case study. *Vadose Zone Journal*, **9**, 1025–1033.

Zenone T, Fischer M, Arriga N et al. (2015) Biophysical drivers of the carbon dioxide, water vapor, and energy exchanges of a short-rotation poplar coppice. *Agricultural and Forest Meteorology*, **209**, 22–35.

Zona D, Janssens IA, Aubinet M, Gioli B, Vicca S, Fichot R, Ceulemans R (2013) Fluxes of the greenhouse gases ($CO_2$, $CH_4$ and $N_2O$) above a short-rotation poplar plantation after conversion from agriculture land. *Agricultural and Forest Meteorology*, **169**, 100–110.

Zsuffa L, Giordano E, Pryor LD, Stettler RF (1996) Trends in poplar-culture: some global and regional perspectives. In: *Biology of Populus and its Implications for Management and Conservation* (eds Stettler RF, Bradshaw HD, Heilman PE, Hinckley TM), pp. 515–539. National Research Council, Research Press, Ottawa, Canada.